Springer

Acta Mechanica Sinica

CrossMark click for updates

•RESEARCH PAPER•

Acta Mech. Sin., Vol. 39, 122231 (2023)
https://doi.org/10.1007/s10409-022-22231-x

The initiation characteristics of oblique detonation in acetylene-air mixtures in the finite wedge

Yichen Zhang[1], Gaoxiang Xiang[1,2*], Qirong Tu[1], Qiu Wang[3], and Haotian Wei[4]

[1] *School of Mechanics, Civil Engineering & Architecture, Northwestern Polytechnical University, Xi'an 710129, China;*
[2] *Research & Development Institute of Northwestern Polytechnical University in Shenzhen, Shenzhen 518057, China;*
[3] *State Key Laboratory of High Temperature Gas Dynamics, Institute of Mechanics, Chinese Academy of Sciences, Beijing 100190, China;*
[4] *School of Astronautics, Northwestern Polytechnical University, Xi'an 710129, China*

Received July 24, 2022; accepted July 29, 2022; published online September 29, 2022

Oblique detonation waves (ODWs) have been widely studied due to their application in hypersonic propulsion. Most of the previous studies focus on hydrogen fuel, and the induced wedge is always infinite. In this paper, based on the detailed chemical reaction model, the two-dimensional multi-component Euler equations are solved, and the finite wedge-induced oblique detonations for acetylene-air mixtures are investigated numerically and theoretically. Effects of expansion waves, inflow Mach number and equivalence ratio (ER) on initiation characteristics of ODW are studied according to the initiation criterion in the confined space. Results show that the initiation distance of acetylene is relatively larger than the hydrogen fuel, and the convergence position of deflagration waves and the originated position of expansion waves determine the initiation characteristics of ODW. As the originated position of the expansion wave is downstream of the convergence position of the deflagration, the ODW is ignited; Otherwise, the ODW is not initiated. The characteristics length of induction zone presents a U-shaped curve distribution for different ERs, both fuel-rich and lean-burn conditions will result in the non-initiation of ODW.

Acetylene, Finite wedge, Oblique detonation, Initiation characteristics, Equivalence ratio

Citation: Y. Zhang, G. Xiang, Q. Tu, Q. Wang, and H. Wei, The initiation characteristics of oblique detonation in acetylene-air mixtures in the finite wedge, Acta Mech. Sin. **39**, 122231 (2023), https://doi.org/10.1007/s10409-022-22231-x

1. Introduction

Detonation waves have high thermal cycle efficiency, fast heat release rate, and crucial potential application in hypersonic propulsion [1,2]. The detonation engines based on detonation combustion include rotating detonation engine (RDE), pulse detonation engine (PDE) and oblique detonation engine (ODE). The ODE is suitable for the air-breathing hypersonic vehicles due to its advantages of low flight resistance, light weight, simpler structure, fast energy release and wide range of flight Mach number, attracting wide attention of researchers [3-11]. However, the research on ODE is still basic. It is of great significance to study the initiation mechanism of ODE in practical flow.

For the past several decades, oblique detonation waves (ODWs) have been researched extensively, including their wave structures and transformation characteristics [12-26], initiation mechanism and stationary characteristics [27-34]. Li et al. [12] found that the ODW structure consists of the oblique shock wave (OSW), induction zone, deflagration waves and the ODW. Subsequently, Viguier et al. [13], Desbordes et al. [14], and Kamel et al. [15] observed these wave configurations through their experimental investigations. Teng et al. and Miao et al. [16,17] showed that there are two transition structures: the abrupt transition and the smooth transition, from the oblique shock surface to the oblique detonation surface. Liu et al. [18] presented the existence of hysteresis phenomena in ODW: the hysteresis of abrupt to smooth configuration and the hysteresis of upstream and downstream. Further, researchers study the ef-

*Corresponding author. E-mail address: xianggx@nwpu.edu.cn (Gaoxiang Xiang)
Executive Editor: Zhenhua Xia

fects of characteristic parameters on the flow field of ODW. Yang et al. [19] indicated that inflow Mach number impacts oblique detonation initiation. With the inflow Mach number increasing, the initiation position moved upward, and the transition structure changed from mutation type to stable type. Liu et al. [20] investigated the ODW at low inflow Mach number, and found that the decreasing inflow Mach number and increasing wedge angle are conducive to upstream propagation of the ODW. Xiang et al. [3], Fang et al. [27], and Chen et al. [28] studied the influence of equivalence ratio (ER) on initiation characteristics and show that high or low ER will make the initiation length of ODW increase. Many scholars research the initiation mechanism and stationary characteristics of ODW. Lin et al. [29] found that when the wedge angle is greater than the critical angle, the ODW will be detached, the detached detonation wave will be unstable, and it will be extinct and re-ignited.

Most of the previous studies based on the infinite wedge and the effects of expansion waves in confined space are not taken into consideration. While in the conditions of real flow, the wedge is finite and the space is confined; the OSW, ODW, slip lines, expansion waves, and their interference with the boundary layer influence the flow field characteristics of ODW [35]. In addition, the current researches focus on hydrogen fuel, but it has the disadvantages of high production cost and difficulty in storage. Therefore, it is necessary to consider the initiation mechanism of oblique detonation with other fuels, such as aviation kerosene and hydrocarbon fuel [36-44]. Acetylene is widely used in the research of oblique detonation [36,37], because it is stable and easy to detonate, and the detonation structure is regular. Fang et al. [36] and Zhang et al. [37] simulated the initiation of acetylene-oxygen in argon dilution, and studied the wave system structure and initiation characteristics of the ODW induced by acetylene. In summary, the research on ODW based on hydrocarbon fuels needs to be carried out urgently.

In this paper, based on the detailed chemical reactions, the initiation mechanism of oblique detonation based on premixed acetylene-air mixtures for a finite wedge is studied by solving the two-dimensional (2D) Euler equations. Section 2 introduces the mathematical and physical model. In Sect. 3, the initiation mechanism of oblique detonation based on acetylene-air mixtures at different Mach numbers and ERs is investigated, and the theoretical analysis of constant volume combustion (CVC) theory is presented. Section 4 gives the conclusion of this paper.

2. Physical and mathematical models

Figure 1 is the schematic diagram of the oblique detonation induced by a finite wedge. The OSW induced by the wedge occurs first in the hypersonic combustible inflow. For a high

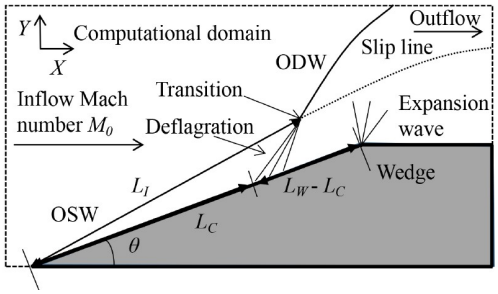

Figure 1 Sketch of the oblique detonation simulation.

inflow Mach number causing a high post-shock temperature behind the OSW, an exothermic chemical reaction begins. The deflagrations converge at the front of the wedge, leading to the formation of the ODW. The expansion waves are generated at the front end of the horizontal wedge. The dark zone is the solid wall with an 18° wedge angle. The wall does not consider viscosity, and dashed line on the right is the outflow condition, and the dashed line above is the far-field condition. The zone bounded by the dashed line and the dark area's upper boundary is the entire computational zone.

In this paper, the flight Mach number is selected as 9, 10 and 11. The initial flight parameters are the standard atmospheric parameters at an altitude of 30 km (T_0 = 226.51 K, P_0 = 1197 Pa). The inflow parameters are compressed by a two-stage wedge surface of 9° before it enters the combustion chamber. Stoichiometric acetylene, oxygen, and nitrogen mixtures, i.e., $C_2H_2 : O_2 : N_2 = \alpha : 1 : 3.76$, are used in which α is decided by ER and ranges from 0.4 to 1.7 in this study. The oblique wedge's length is defined as the length of the wedge and denoted as L_W. The size of the L_W is given in each section and indicated in the associated figures. The length from the leading wedge point to the front point of ODW is defined as the characteristic length of the induction zone and designated as L_I. The length from the leading wedge point to the front point of the deflagration wave is defined as another characteristic length of the induction zone and marked as L_C.

In this paper, the influence of viscosity is not considered, so the 2D multi-component Euler equations considering elementary reactions [3,35,36] are solved, i.e.,

$$\frac{\partial U}{\partial t}+\frac{\partial F}{\partial x}+\frac{\partial G}{\partial y}=S, \tag{1}$$

where

$$U=\begin{Bmatrix}\rho_1\\ \vdots\\ \rho_n\\ \rho u\\ \rho v\\ e\end{Bmatrix}, F=\begin{Bmatrix}\rho_1 u\\ \vdots\\ \rho_n u\\ \rho u^2+p\\ \rho uv\\ (e+p)u\end{Bmatrix}, G=\begin{Bmatrix}\rho_1 v\\ \vdots\\ \rho_n v\\ \rho uv\\ \rho v^2+p\\ (e+p)v\end{Bmatrix}, S=\begin{Bmatrix}\dot{\omega}_1\\ \vdots\\ \dot{\omega}_n\\ 0\\ 0\\ 0\end{Bmatrix}. \tag{2}$$

In Eq. (2), the subscript i (i = 1, 2, ⋯, n) refers to the i-th substances. The total specific energy e and total density ρ can be determined by

$$\rho = \sum_{i=1}^{n} \rho_i, \; e = \rho h - p + \frac{1}{2}\rho(u^2 + v^2), \tag{3}$$

where u is the velocity in the x-direction and v is the velocity in the y-direction. h is the specific enthalpy, which is defined as $h = \sum_{i=1}^{n} \rho_i h_i / \rho$. The equation of state is $p = \sum_{i=1}^{n} \rho_i \frac{R_0}{\omega_i} T$, R_0 is the gas constant, and ω_i is the molecular weight of the i-th species.

In this study, the chemical kinetic model is an acetylene-oxygen chemical mechanism [45], which can be used for numerical simulation of oblique detonation [36]. Similar to the study conducted by Xiang et al. [3,35,46], in this study, the AUSMPW+ scheme [47], which is beneficial to capture shock waves and obtain quantitative results, is used to discretize the governing equations. To avoid the influence of the grid size scale on numerical simulation results, a resolution study on the grid size scale is performed. In the numerical simulation of 2D oblique detonation, the resolution study is usually performed with the double refinement of the grid size [16]. In this paper, two sets of grid sizes, 0.2 mm × 0.2 mm and 0.1 mm × 0.1 mm at M_0 = 9, L_W = 180 mm and ER = 1.0 are compared. Figure 2a shows the comparison of temperature contour based on two different sets of grid sizes. The temperature contours of ODW based on two distinct grid sizes are basically the same, illustrating a typical structure with the abrupt transition. In Fig. 2b, the temperature and pressure distributions of wall boundary based on two different grid sizes are presented. The solid line and dotted line for two sets of grid size completely coincide with each other. Therefore, the numerical results indicate that the grid size scale has almost no effect on the flow field of ODW. In this paper, the grid size of 0.2 mm × 0.2 mm is used for numerical simulation.

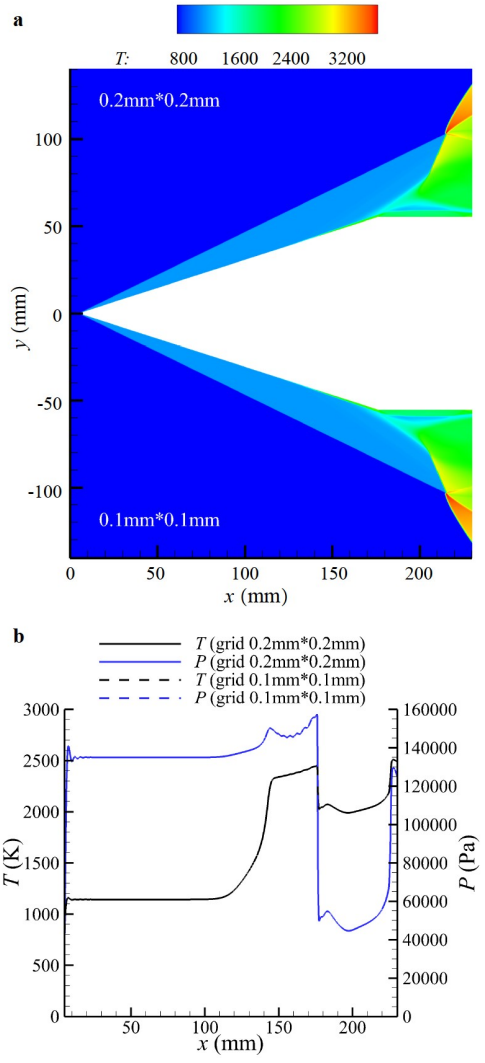

Figure 2 Comparison diagram based on two different grid sizes. **a** Temperature contour of ODW; **b** temperature and pressure distributions of wall.

3. Result and discussion

3.1 Theoretical verification

Previous studies have investigated the ODW structure and found that ODW has two initiation mechanisms. One is chemical kinetics-controlled and the other is wave- (or gas-dynamics-) controlled [48]. The initiation mechanism is determined by analyzing the fluid elements near the wedge surface. In the chemical kinetics-controlled one, detonation combustion is close to CVC, so the characteristic length of the induction zone can be predicted by the CVC theory. CVC theory refers to the theory of the combustion of fuel and oxygen under the condition that the volume remains constant (or substantially constant). For example, the combustion process of fuel in the combustion chamber of an internal combustion engine or a jet engine is basically close to CVC and is suitable for the CVC theory. However, in the wave-controlled one, the initiation length of the induction zone calculated by CVC theory is longer than the actual length of the induction zone. And there is a lack of theoretical methods for predicting the initiation length of the induction zone in this control condition. Therefore, researchers often use CVC theory to identify the initiation mechanism of ODW and determine the accuracy of numerical simulation [36,37].

As there are no published experimental results for ODW in acetylene-air mixtures, the numerical results are compared with theoretical results of the CVC theory. For the CVC theory, the flow behind the oblique shock is assumed as ideal, and the mixture is burned completely [36,49]. First, through numerical simulation and shock relationship, we can

obtain the post-oblique-shock species densities, temperature and particle velocity. Then, the post-oblique-shock temperature and species densities are used to simulate CVC to obtain the reaction time required to attain a mixture with a 10% increase from the post-shock value. The calculations are performed using the CHEMKIN package [49]. Finally, the theoretical initiation length L_C is deduced by multiplying the post-oblique-shock particle velocity with the reaction time. Despite the simplicity of the formulation, this analysis provides a prediction method for the general structure of ODW [36,48,49].

Figure 3 shows the comparison between the theoretical results solved by CVC theory and the numerical results. The squares and solid lines represent theoretical results, and the diamonds and dotted lines mean theoretical results. There is little difference between the theoretical value and the simulated value, and the error is less than 10%. The theoretical results are in good agreement with the simulation results, indicating that the initiation mechanism is chemical kinetics-controlled. Theoretical results also show that the initiation lengths L_C depend on the ER. Within a range of equivalent ratios, the characteristic length of the induction zone forms a U-shaped curve. Similar to the conclusion of the study in Sect. 3.3 and previous studies [3,24,25], theoretical results of CVC theory indicate that both high equivalent ratio and low equivalent ratio can make the initiation distance of the ODW longer and not be ignited.

3.2 Effects of expansion waves on ODW

Figure 4 presents the ODW structure induced by a finite wedge at different M_0 and L_W when ER = 1.0. In this paper, numerical results show that this transition pattern is the abrupt transition, one of the two transition patterns from OSW to ODW determined in previous studies [16,17]. Compared with the previous results [11-15], the wave structure of the finite wedge is the same as that of the infinite wedge (Fig. 4a and b). To obtain the critical detonation limits of the wedge length, L_W is shortened until it fails to detonate. After the inflection point, the expansion waves formed make the temperature drops sharply, which causes the detonation is not ignited for smaller L_W at M_0 = 9 and 11 (Fig. 4c and d). The temperature and pressure could not reach the conditions of initiation; the oblique detonation failed to detonate. Results indicate that the critical characteristic length L_W from the detonation to no-detonation is 164 mm, 57 mm and 30 mm at M_0 = 9, 10 and 11. As the wedge length L_W is more minor than these characteristic lengths, the ODW is not ignited; otherwise, the ODW is ignited [50]. In addition, numerical results also confirm that the initiation position moves upstream with the increasing inflow Mach number M_0 [19]. Figure 5 shows the variation of pressure and temperature of flow field on wall boundary for Fig. 4, the dotted line represents the change of temperature in the flow field, and the solid line shows the change of pressure in the flow field. The blue line presents the temperature and pressure trend without detonation, and the black line indicates the temperature and pressure trend with detonation. In Fig. 5, due to the compression by the OSW, the temperature and pressure of the inflow gas increase suddenly. In the induced zone, the temperature and pressure on the wall boundary continue to rise. Finally, the temperature and pressure after the inflection point sharply decrease due to the influence of the expansion wave.

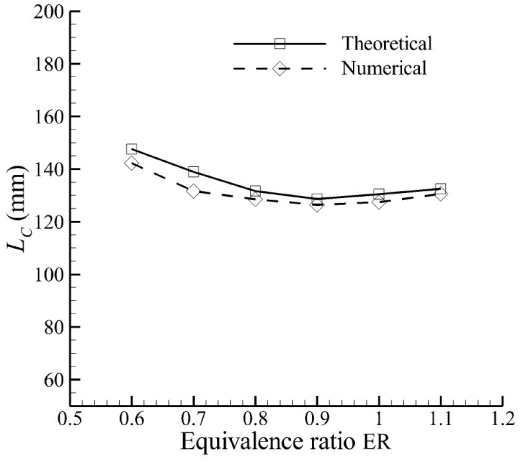

Figure 3 Numerical vs. theoretical L_C at M_0 = 9 and L_W = 180 mm.

Figure 6 shows the influence of L_W on the initiation characteristic of ODW at different ERs. The horizontal coordinate-axis ER is the ER, and the ordinate-axis L_W is the length from the leading wedge to the inflection point. The red circle icon indicates detonations; the white circle icon represents no detonations. As shown in Fig. 6a, at M_0 = 9 and L_W = 200 mm, the range of equivalent ratios that can initiate the oblique detonation successfully is 0.4 to 1.7. As the length of wedge is reduced to L_W = 190 mm, the range of equivalent ratios for detonations is 0.5 to 1.5. When the wedge length continues to decrease to L_W = 180 mm, the range of equivalent ratios for detonations is only 0.6 to 1.1. The fuel-rich and lean-burn conditions result in the increase of the initiation distance and make the ODW not be ignited. As shown in Fig. 6b and c, at M_0 = 10 and M_0 = 11, the decreasing of L_W decreases the scope of detonations. The expansion waves cause the temperature and pressure of the gas to drop. If the temperature and pressure are too low, the hotspot in the flow field is not triggered and no detonations will occur. Therefore, the existence of expansion waves has a negative effect on oblique detonation initiation.

3.3 Effects of ER on ODW

To study the impact of ERs on ODW, M_0 = 9 and L_W = 180 mm are kept unchanged. For different equivalent ratios,

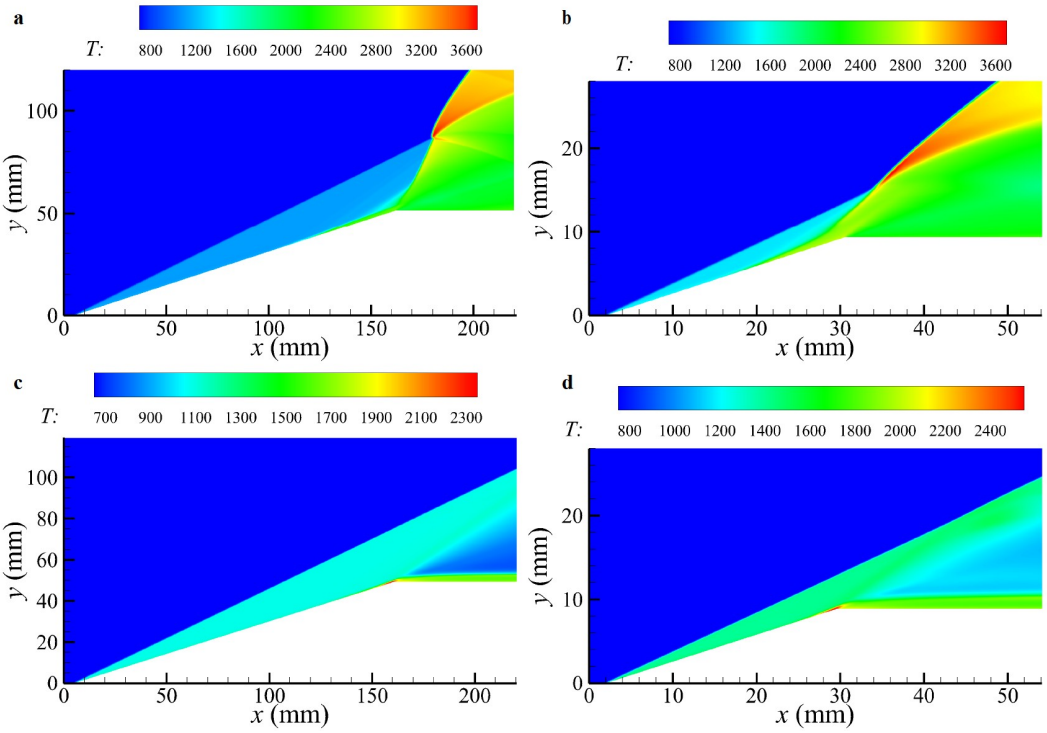

Figure 4 Temperature fields of ODW at ER = 1.0. **a** M_0 = 9, L_W = 164 mm; **b** M_0 = 11, L_W = 30 mm; **c** M_0 = 9, L_W = 163 mm; **d** M_0 = 11, L_W = 29 mm.

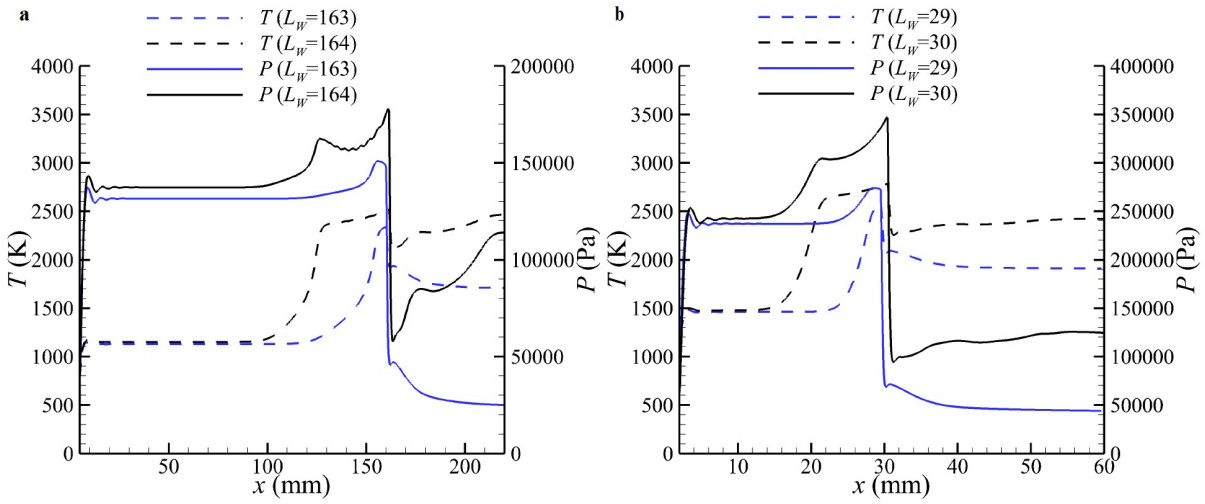

Figure 5 Temperature and pressure distributions of wall boundary. **a** M_0 = 9; **b** M_0 = 11.

ODW temperature profile is shown in Fig. 7. The equivalent ratio has an excellent influence on the initiation of oblique detonation. As the ER is changed from 0.4 to 0.7, the initiation mode of ODW transforms from no-initiation to initiation (Fig. 7a and b). As the equivalent ratio increases to ER = 0.9 (Fig. 7c) and ER = 1.0 (Fig. 7d) further, the characteristic length of induction zone L_I gets shorter but becomes longer at the stoichiometric mixture of ER = 1.1 (Fig. 7e). Figure 7f shows that as the equivalent ratio increases to ER = 1.2, the ODW is not initiated again. In combustion sciences, the rate of reaction is proportional to the concentration of reactants [51]. In this paper, it can be understood that when the ER is too high or too low, the mole fraction of acetylene or oxygen is too low, resulting in a slower rate of reaction. And because the length of the induction zone is related to the combustion rate, the detonation distance of ODW is different in different ERs. Therefore, when the equivalent ratio is too low or too high, the fuel-rich and lean-burn increase the initiation distance in the confined space, and lead to the no-initiation of the ODW.

Figure 8 shows the temperature and the pressure on the wall boundary with different ERs. The solid line and dotted lines represent the change of temperature and pressure in the flow field. The black line, blue lines and red lines show the

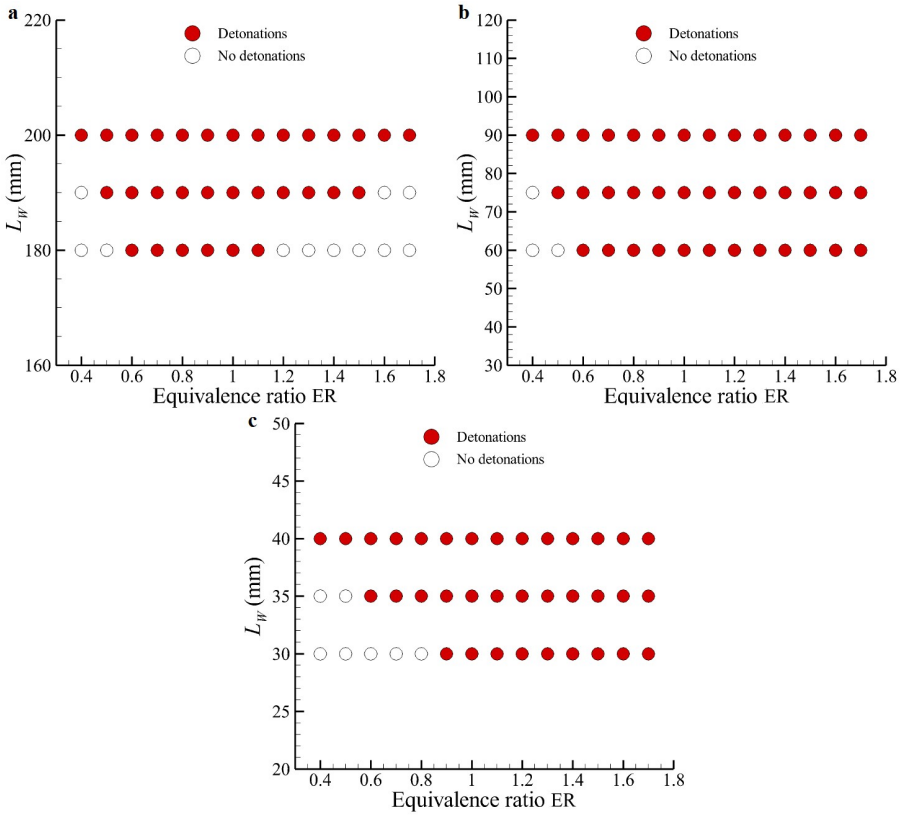

Figure 6 Initiation characteristic of ODW at different L_W and ER. **a** M_0 = 9; **b** M_0 = 10; **c** M_0 = 11.

temperature and pressure trend at ER = 0.7, ER = 0.9 and ER = 1.1 respectively. The change of equivalent ratios at constant velocity affects the numerical value of gas constant, and then affects shock relation for solving the temperature ratio. Therefore, the different ERs lead to different temperatures [3]. And theoretically, the rate of combustion increases with the increase of temperature [51], which further changes the length of the induction zone. As shown in Fig. 8, the oblique wedge induced the oblique shock, and the temperature and pressure in front of the wedge rose sharply. From the front point of the wedge to the front of the induction region, the temperature and pressure are basically unchanged. After the induction zone, the temperature and pressure rise sharply. The temperature changes obviously at three different equivalent ratios. When ER = 1.1, the maximum temperature at the end of the wedge reaches 2500 K. However, when ER = 0.9 and 0.7, the temperature at the same position is only about 2350 K and 2150 K. Eventually, the expansion waves originated from the inflection point between the oblique and the horizontal wedge result in the temperature and pressure decrease.

To visually display the effects of equivalent ratio on ODW, Fig. 9 shows the characteristic length of induction zone with different equivalent ratios. In Fig. 9a, the oblique detonation will not be ignited as the equivalent ratio is too high or too low. Within the range of equivalent ratios from 0.6 to 1.1, the oblique detonation is initiated, and the variation trend of the characteristic length of the induction zone presents a U-shaped curve. Figure 9b is another numerical result at M_0 = 11, L_W = 30 mm. As the ER increases from 1.0 to 1.7, the length of induction zone L_I changes slightly. It is different from the result we expected and the conclusion of previous studies [3,27,28]. It is worth mentioning that the length of the induction zone at M_0 = 9 is about six times that at M_0 = 11. In the same confined space, the oblique detonation at a higher Mach number with a shorter initiation distance is easy to be ignited and has a wider initiation range. The location of the originated expansion waves L_W and the convergence location of the deflagrations L_C determine the initiation characteristics of the ODW in confined space. As $L_C < L_W$, the ODW is initiated. On the contrary, the ODW is not ignited. In terms of combustion mechanism, the combustion rate reaches the maximum when the ER is around ER = 1 [51]. The variation of the combustion rate with the ER presents an inverted U-shaped curve [51]. The length of the ODW induction zone was inversely proportional to the rate of combustion, so the change of L_I with ER showed a U-shaped curve. It shows that the simulation results are consistent with the theory.

4. Conclusion

In this paper, a detailed chemical model is used to solve the

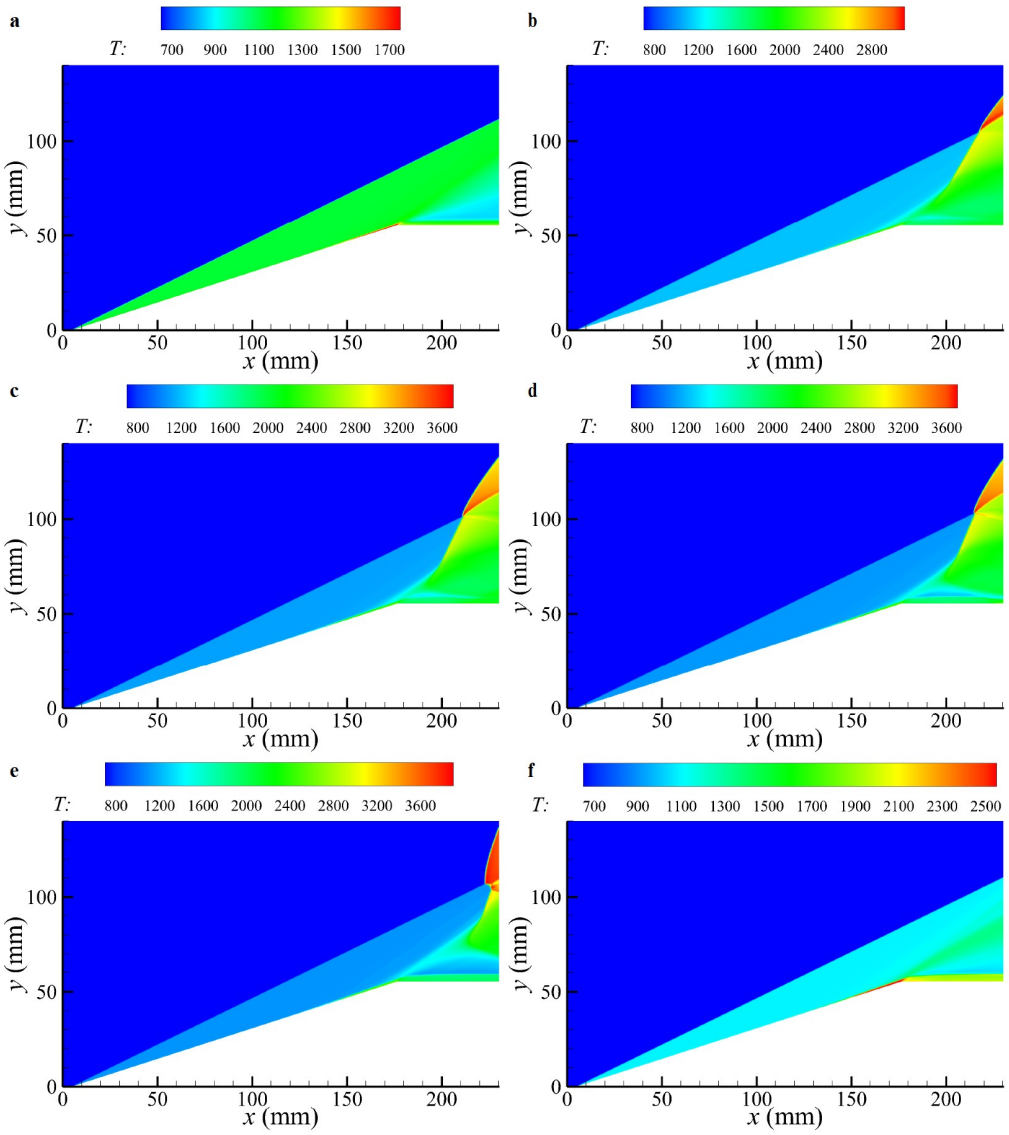

Figure 7 Temperature contour of ODW with different ER at $M_0 = 9$ and $L_W = 180$ mm. **a** ER = 0.4; **b** ER = 0.7; **c** ER = 0.9; **d** ER = 1.0; **e** ER = 1.1; **f** ER = 1.2.

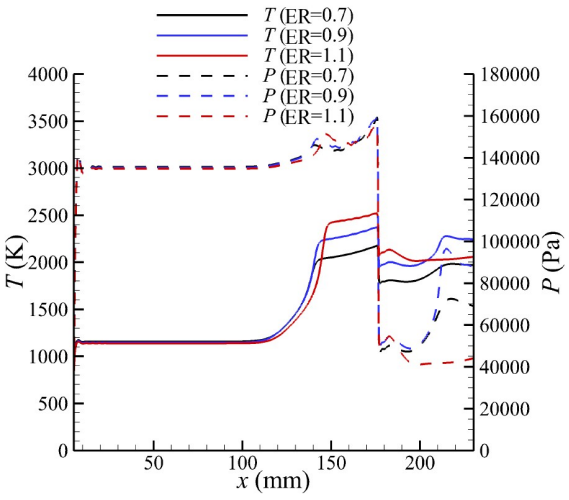

Figure 8 Temperature and pressure distributions on wall boundary with different ER at $M_0 = 9$ and $L_W = 180$ mm.

2D multicomponent Euler equation [3,27,28,46]; the flow field characteristics of ODW for an acetylene-air mixture in the confined space are investigated. The effects of expansion waves with different wedge length L_W and ERs on the wave structures, induction zone, initiation characteristics and flow field parameters are studied in detail. The theoretical length of the induction zone is obtained by CVC theory and has good agreement with numerical results. The expansion waves have a significant influence on the initiation of oblique detonation. It decreases the temperature and pressure of the inflow gas and restrains the formation of the hot spots for oblique detonation. As the location of the expansion waves is upstream of the deflagration waves, the ODW is not ignited; On the contrary, the ODW is initiated. The characteristics length of induction zone presents a U-shaped curve distribution for different ERs, both fuel-rich in high ER and lean-burn in low ER will result in the non-initiation of ODW.

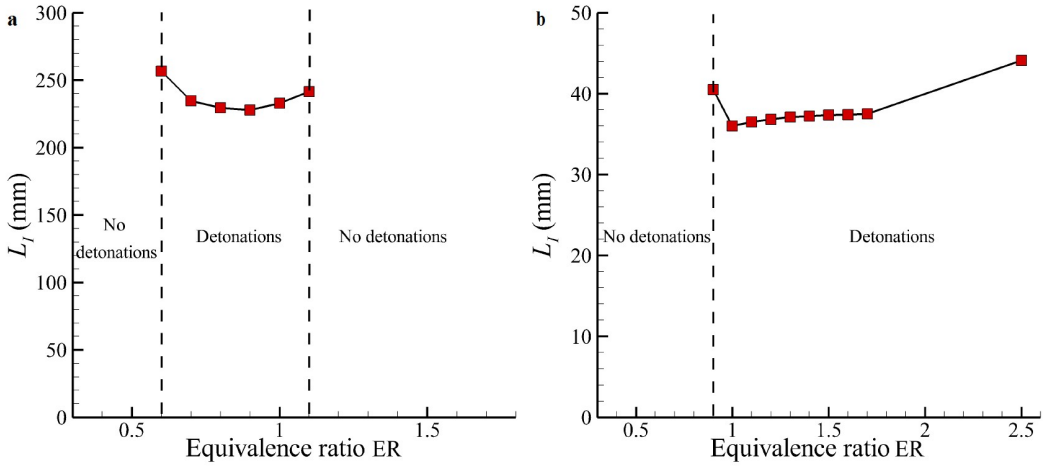

Figure 9 Effects of ER on characteristic length of induction zone. **a** M_0 = 9, L_W = 180 mm; **b** M_0 = 11, L_W = 30 mm.

The higher the inflow Mach number, the wider the initiation range of the ODW in the confined space. This paper provides a significant basis for the research of hydrocarbon-fuel ODE in confined space.

Author contributions *Yichen Zhang wrote the first draft of the manuscript, conducted the numerical simulations. Gaoxiang Xiang designed the research, conceptualization, review and editing. Qirong Tu, Qiu Wang and Haotian Wei conducted the literature research and helped organize the manuscript.*

Acknowledgements *This work was supported by the Guangdong Basic and Applied Basic research Foundation (Grant No. 2022A1515011565), Foundation of State Key Laboratory of High Temperature Gas Dynamics (Grant No. 2021KF10), and the China Postdoctoral Science Foundation (Grant Nos. 2021M692633 and 2022T150534).*

1 Z. Jiang, Z. Zhang, Y. Liu, C. Wang, and C. Luo, Criteria for hypersonic airbreathing propulsion and its experimental verification, Chin. J. Aeronauti. **34**, 94 (2021).
2 Z. Jiang, Z. Hu, Y. Wang, and G. Han, Advances in critical technologies for hypersonic and high-enthalpy wind tunnel, Chin. J. Aeronauti. **33**, 3027 (2020).
3 G. Xiang, H. Li, R. Cao, and X. Chen, Study of the features of oblique detonation induced by a finite wedge in hydrogen-air mixtures with varying equivalence ratios, Fuel **264**, 116854 (2020).
4 Z. Jiang, and H. Yu, Theories and technologies for duplicating hypersonic flight conditions for ground testing, Natl. Sci. Rev. **4**, 290 (2017).
5 J. H. S. Lee, The Detonation Phenomenon (Cambridge University Press, Cambridge, 2008).
6 G. Xiang, X. Gao, X. Jie, X. Li, H. Li, and X. Chen, Flowfield characteristics in sidewall compression inlets, Acta Mech. Sin. **36**, 678 (2020).
7 C. K. Yuan, K. Zhou, Y. F. Liu, Z. M. Hu, and Z. L. Jiang, Spectral measurements of hypervelocity flow in an expansion tunnel, Acta Mech. Sin. **35**, 24 (2019).
8 G. Xiang, C. Wang, H. Teng, Y. Yang, and Z. Jiang, Study on Mach stems induced by interaction of planar shock waves on two intersecting wedges, Acta Mech. Sin. **32**, 362 (2016).
9 B. Zhang, Y. Li, and H. Liu, Analysis of the ignition induced by shock wave focusing equipped with conical and hemispherical reflectors, Combust. Flame **236**, 111763 (2022).
10 B. Zhang, Y. Li, and H. Liu, Ignition behavior and the onset of quasi-detonation in methane-oxygen using different end wall reflectors, Aerosp. Sci. Tech. **116**, 106873 (2021).
11 C. K. Yuan, and Z. L. Jiang, Experimental investigation of hypersonic flight-duplicated shock tunnel characteristics, Acta Mech. Sin. **37**, 422 (2021).
12 C. Li, K. Kailasanath, and E. S. Oran, Detonation structures behind oblique shocks, Phys. Fluids **6**, 1600 (1994).
13 C. Viguier, L. F. F. Silva, D. Desbordes, and B. Deshaies, Onset of oblique detonation waves: Comparison between experimental and numerical results for hydrogen-air mixtures, Symposium (Int.) Combust. **26**, 3023 (1996).
14 D. Desbordes, L. Hamada, and C. Guerraud, Supersonic H_2-air combustions behind oblique shock waves, Shock Waves **4**, 339 (1995).
15 M. R. Kamel, C. I. Morris, I. G. Stouklov, and R. K. Hanson, PLIF imaging of hypersonic reactive flow around blunt bodies, Symposium (Int.) Combust. **26**, 2909 (1996).
16 H. H. Teng, and Z. L. Jiang, On the transition pattern of the oblique detonation structure, J. Fluid Mech. **713**, 659 (2012).
17 S. Miao, J. Zhou, S. Liu, and X. Cai, Formation mechanisms and characteristics of transition patterns in oblique detonations, Acta Astronaut. **142**, 121 (2017).
18 Y. Liu, L. Wang, B. Xiao, Z. Yan, and C. Wang, Hysteresis phenomenon of the oblique detonation wave, Combust. Flame **192**, 170 (2018).
19 P. Yang, H. Teng, Z. Jiang, and H. D. Ng, Effects of inflow Mach number on oblique detonation initiation with a two-step induction-reaction kinetic model, Combust. Flame **193**, 246 (2018).
20 Y. Liu, D. Wu, S. Yao, and J. Wang, Analytical and numerical investigations of wedge-induced oblique detonation waves at low inflow Mach number, Combust. Sci. Tech. **187**, 843 (2015).
21 H. Teng, Y. Zhang, P. Yang, and Z. Jiang, Oblique detonation wave triggered by a double wedge in hypersonic flow, Chin. J. Aeronauti. **35**, 176 (2022).
22 Y. Gao, H. Li, G. Xiang, and S. Peng, Initiation characteristics of oblique detonation waves from a finite wedge under argon dilution, Chin. J. Aeronauti. **34**, 81 (2021).
23 H. Li, J. Li, C. Xiong, W. Fan, L. Zhao, and W. Han, Investigation of hot jet on active control of oblique detonation waves, Chin. J. Aeronauti. **33**, 861 (2020).
24 Q. Qin, and X. Zhang, Study on the transition patterns of the oblique detonation wave with varying temperature of the hydrogen-air mixture, Fuel **274**, 117827 (2020).
25 B. Zhang, H. Liu, and Y. Li, The effect of instability of detonation on the propagation modes near the limits in typical combustible mixtures, Fuel **253**, 305 (2019).
26 B. Zhang, and H. Liu, Theoretical prediction model and experimental

investigation of detonation limits in combustible gaseous mixtures, Fuel **258**, 116132 (2019).
27 Y. Fang, Z. Hu, H. Teng, Z. Jiang, and H. D. Ng, Numerical study of inflow equivalence ratio inhomogeneity on oblique detonation formation in hydrogen-air mixtures, Aerosp. Sci. Tech. **71**, 256 (2017).
28 N. Chen, S. A. Esfehani, S. Bhattrai, Y. Liu, and H. Tang, Numerical study on effects of equivalence ratio on initiation characteristics of oblique detonation waves, J. Propuls. Technol. **39**, 2798 (2018).
29 Z. Lin, J. Zhou, J. Zhang, and Y. Wang, Investigation of detached detonation induced by oblique shock in premixed supersonic flow, J. Aerosp. Power **1**, 56 (2009).
30 G. Xiang, Y. Zhang, C. Zhang, and Y. Kou, Study on initiation mechanism of oblique detonation induced by blunt bump on wedge surface, Fuel **323**, 124314 (2022).
31 Y. Fang, Z. Zhang, and Z. Hu, Effects of boundary layer on wedge-induced oblique detonation structures in hydrogen-air mixtures, Int. J. Hydrogen Energy **44**, 23429 (2019).
32 G. X. Xiang, X. Gao, W. J. Tang, X. Z. Jie, and X. Huang, Numerical study on transition structures of oblique detonations with expansion wave from finite-length cowl, Phys. Fluids **32**, 056108 (2020).
33 G. Xiang, Y. Zhang, Q. Tu, Y. Gao, X. Huang, and T. Peng, The initiation characteristics of oblique detonation waves induced by a curved surface, Aeros. Sci. Tech. **128**, 107743 (2022).
34 B. Zhang, The influence of wall roughness on detonation limits in hydrogen-oxygen mixture, Combust. Flame **169**, 333 (2016).
35 G. Xiang, H. Li, G. Zhang, X. Xie, and Y. Zhang, Characteristics of the oblique detonation flow field induced by a complex wave structure, Int. J. Hydrogen Energy **46**, 17435 (2021).
36 Y. Fang, Y. Zhang, X. Deng, and H. Teng, Structure of wedge-induced oblique detonation in acetylene-oxygen-argon mixtures, Phys. Fluids **31**, 026108 (2019).
37 Y. Zhang, Y. Fang, H. D. Ng, and H. Teng, Numerical investigation on the initiation of oblique detonation waves in stoichiometric acetylene-oxygen mixtures with high argon dilution, Combust. Flame **204**, 391 (2019).
38 L. Wang, H. Ma, Z. Shen, B. Xue, Y. Cheng, and Z. Fan, Experimental investigation of methane-oxygen detonation propagation in tubes, Appl. Thermal Eng. **123**, 1300 (2017).
39 Y. Wang, J. Le, C. Wang, and Y. Zheng, A non-premixed rotating detonation engine using ethylene and air, Appl. Thermal Eng. **137**, 749 (2018).
40 B. Zhang, Detonation limits in methane-hydrogen-oxygen mixtures: Dominant effect of induction length, Int. J. Hydrogen Energy **44**, 23532 (2019).
41 B. Zhang, H. Liu, B. Yan, and H. D. Ng, Experimental study of detonation limits in methane-oxygen mixtures: Determining tube scale and initial pressure effects, Fuel **259**, 116220 (2020).
42 B. Zhang, X. Chang, and C. Bai, End-wall ignition of methane-air mixtures under the effects of CO_2/Ar/N_2 fluidic jets, Fuel **270**, 117485 (2020).
43 B. Zhang, H. Liu, and B. Yan, Effect of acoustically absorbing wall tubes on the near-limit detonation propagation behaviors in a methane-oxygen mixture, Fuel **236**, 975 (2019).
44 B. Zhang, and H. D. Ng, An experimental investigation of the explosion characteristics of dimethyl ether-air mixtures, Energy **107**, 1 (2016).
45 B. Varatharajan, and F. A. Williams, Chemical-kinetic descriptions of high-temperature ignition and detonation of acetylene-oxygen-diluent systems, Combust. Flame **124**, 624 (2001).
46 G. Xiang, Y. Zhang, X. Gao, H. Li, and X. Huang, Oblique detonation waves induced by two symmetrical wedges in hydrogen-air mixtures, Fuel **295**, 120615 (2021).
47 K. H. Kim, C. Kim, and O. H. Rho, Methods for the accurate computations of hypersonic flows, J. Comput. Phys. **174**, 38 (2001).
48 H. Teng, H. D. Ng, and Z. Jiang, Initiation characteristics of wedge-induced oblique detonation waves in a stoichiometric hydrogen-air mixture, Proc. Combust. Inst. **36**, 2735 (2017).
49 R. J. Kee, F. M. Rupley, E. Meeks, and J. A. Miller, CHEMKIN-III: A fortran chemical kinetic package for the analysis of gas-phase chemical and plasma knietics, Technical Report (Sandia National Labs, Livermore, 1996).
50 G. Xiang, X. Li, X. Sun, and X. Chen, Investigations on oblique detonations induced by a finite wedge in high altitude, Aerosp. Sci. Tech. **95**, 105451 (2018).
51 S. R. Turns, An Introduction to Combustion: Concepts and Applications (McGraw-Hill Companies, New York, 2000).

乙炔-空气混合物中有限长楔面诱导斜爆轰波的起爆特性

张益晨, 项高翔, 涂启荣, 汪球, 魏浩天

摘要 斜爆轰波在高超声速推进具有重要的应用潜力, 受到了研究者们的广泛研究. 以往的研究, 大多基于氢气燃料, 且楔面总是无限长的. 本文基于详细的化学反应模型, 通过求解二维考虑基元反应的多组分欧拉方程, 对乙炔-空气混合物在有限长楔形面诱导的斜爆轰进行了数值和理论研究. 根据受限空间内的起爆判据, 研究了膨胀波、来流马赫数和当量比对斜爆轰波起爆特性的影响. 结果表明, 乙炔诱导的斜爆轰波的起爆距离相对大于氢燃料诱导的. 爆燃波的会聚位置和膨胀波的产生位置决定了斜爆轰波的起爆特性. 当膨胀波的产生位置在爆燃波会聚位置的下游, 斜爆轰波被点燃; 否则, 斜爆轰波不会起爆. 诱导区特征长度在不同当量比下呈U型曲线分布, 无论是富燃还是贫燃都会导致斜爆轰波不起爆.